UARI Research Report No. 29

HYPERSONIC AERODYNAMIC PROBLEMS
AT RE-ENTRY OF SPACE VEHICLES

by

Rudolf Hermann

Invited lecture presented at the
4. SPACE SYMPOSIUM
at the University of Goettingen, Germany
October 18-22, 1965

UNIVERSITY OF ALABAMA RESEARCH INSTITUTE
Huntsville, Alabama

November 1965

FOREWORD

TABLE OF CONTENTS

LIST OF FIGURES

1.   INTRODUCTION

Today one of the most important aerodynamic problems in astronautics is the return intact of satellites and space vehicles to the earth's surface. This requires a flight through the atmosphere of man-made vehicles with velocities hitherto experienced only by meteors. Particularly in the case of the manned satellites, the requirement of a smooth re-entry with a minimum of deceleration and a minimum of heat transfer to the re-entering vehicle is of great importance. The mechanical energy which a satellite possesses in an orbit near the earth is very large. The kinetic energy alone at circular velocity of 7,910 m/sec near the surface is 3.128×10^7 joules/kg, which is equivalent to 7,470 kcal/kg (ITcal). For comparison, the heat of evaporation for water is about 550 kcal/kg. Hence, if the kinetic energy of a re-entering body would be completely transferred to the body itself, it is obvious that the mass of the body of any known material would be vaporized. Consequently, it is of greatest engineering importance to dissipate as much as possible of this energy into the surrounding medium and to transfer only a small fraction of it to the body itself. To accomplish this, a careful study of the flow processes involved at hypersonic velocities and high temperatures is required.

The re-entering vehicle passes through a large difference in altitudes, and hence encounters a great variation in density and composition of the atmosphere. The strong heating, particularly near the stagnation point, will change considerably the chemical composition of the air flowing along the body. Increasingly high stagnation temperature produces dissociation of the gases and eventually ionization.

During re-entry the Mach number, Reynolds number, Knudsen number, stagnation pressure, stagnation enthalpy, and hence the stagnation temperature, all vary over a wide range. The change in Reynolds number, for instance, indicates the varying influence of viscosity on the flow. At the beginning of re-entry, with comparatively low Reynolds numbers, the influence of viscosity is predominant. As re-entry proceeds, the higher Reynolds numbers signify a decreasing effect of viscosity, until finally the effect of viscosity is restricted to a boundary layer, the dimension of which is small compared with the characteristic body dimension. Decreasing Knudsen number along a re-entry trajectory indicates that the flow is initially in the free molecular regime, passes through the slip flow regime, and finally enters the continuum flow regime.

Before we can calculate the effects caused by the flow, we have to know the environment in its undisturbed condition. Therefore, we will start with a discussion of the environment.

2. PROPERTIES AND COMPOSITION OF THE ATMOSPHERE

Some important properties of the earth's atmosphere are presented in **Figure 1** and **Figure 2**, taken from Reference 1. In Figure 1, left hand side, the density distribution is shown as a function of geometric altitude up to 700 km. Because of the dissociation occurring, we have to distinguish more exactly between the mass density ρ (see Fig. 1) and the number density n, that is, the number of atmospheric particles (atoms or molecules) per unit volume. The variation of number density with geometric altitude is similar to the given mass density.

The temperature T as a function of geometric altitude Z is shown in **Figure 1**, right hand side. Also included is the molecular-scale temperature $T_M = T \cdot M_o/M$. The latter is of importance because rockets and satellites cannot measure temperature directly, but only the ratio T/M. The temperature is then derived as accurately as the average molecular weight, i.e., composition versus altitude, is known.

Figure 2 presents the distribution of molecular weight M, left hand side, and mean free path L, right hand side, with the geometric altitude Z as before. Up to Z=90 km the molecular weight M is taken as constant at 28.96444. Above 90 km, mainly because of molecular dissociation and diffusive separation, the molecular weight changes as depicted.

The mean free path L is the mean value of the distances traveled by each of the neutral particles, in a selected volume, between successive collisions with other particles in that volume. A meaningful average requires that the selected volume be big enough to contain a large number of particles.

With regard to the composition of the atmosphere, the major constituents in lower altitudes are, of course, N_2 and O_2. When we approach altitudes around 90 km, dissociation occurs, and we find a considerable amount of atomic oxygen. Nitrogen dissociation becomes appreciable at higher altitudes, however, it is only slowly increasing. We find that ozone, O_3, has a sharp maximum concentration called the ozone layer at about 30 km altitude (Ref. 2).

The following facts should be emphasized. In higher altitudes the atmosphere at rest has its natural dissociation of oxygen and nitrogen, which should not be confused with the dissociation occurring in the flow around re-entry bodies due to the high stagnation temperature. The latter is an entirely different process and independent of the natural dissociation.

3. RE-ENTRY OF BALLISTIC VEHICLES AND MANNED SPACE CAPSULES INTO THE EARTH'S ATMOSPHERE

At the present time, it is not possible to study and to calculate all phenomena in the complete range of hypersonic high temperature flow problems. Therefore, we must concentrate our efforts on the study of those combinations of variables which are of the greatest engineering concern today. This leads us to the study of hypersonic flow around bodies in the so-called flight corridors. Here certain flight velocities are related to certain flight altitudes, and this relation again depends on the aerodynamic configuration, such as a ballistic capsule or a lifting vehicle, and on the specific area loading of the vehicle. Hence, the knowledge of the re-entry trajectories is a necessity when studying hypersonic flow problems.

3.1 Re-Entry for Ballistic Vehicles

Figure 3 is a typical blunt body configuration used for ballistic vehicles. It is a spherically capped cone which, in high speed flight, generates a detached bow shock. The region between the shock wave and the outer edge of the boundary layer, called the inviscid shock layer, has a subsonic region in the vicinity of the stagnation point; farther downstream the flow is supersonic. Both regions of the inviscid shock layer are separated from the body surface by the boundary layer. Altogether then, there are three distinctly different flow regions, which in general must be analyzed with equally different mathematical methods.

For axisymmetric flow at zero angle of attack, flow fields are symmetric with respect to the body axis; and the inviscid portions can be calculated by presently available methods even though they require considerable computational efforts. If the flow with angle of attack is considered and axial symmetry does not exist, analytical methods are not readily available.

The two types of re-entry which are most frequently analyzed are the ballistic and the lifting vehicle re-entry. Ballistic vehicles, by definition, produce no lift,

hence are in general spherical or capsule type vehicles. The duration of ballistic vehicle re-entry is usually relatively short (in minutes), and thus the flow parameters are typically in a non-steady state. This is particularly true for the heating of the skin. In contrast, the gliding trajectory of a lifting vehicle requires a much longer time, in the order of one hour. Here we will restrict the discussion to only ballistic vehicle flight below 120 km altitude.

Re-entry trajectories for ballistic vehicles from circular orbit around the earth are presented in a velocity-altitude diagram in Figure 4 (Ref. 3). The velocity is made dimensionless by the circular velocity of the earth $u_o = 7,910$ m/s. The trajectories are shown for different values of the ballistic area loading parameter $W/C_D A$, where W is the weight of the vehicle (N), C_D the hypersonic drag coefficient, and A the cross sectional area (m^2). This parameter ranges from 5 to 50,000 N/m^2 and covers the following typical cases (for simplicity $C_D = 1$ assumed) :

$W/C_D A$ (N/m^2)	
5	Light large balloon
500	Small satellite payload
4,000 to 5,000	Re-entry module of Mercury, Gemini,
25,000 to 50,000	ICBM Apollo

From Figure 4 it can be seen that the deceleration of vehicles with small area loading occurs at high altitude, while for vehicles with large area loading the deceleration occurs at lower altitudes. It must be emphasized that all these results have been obtained through simplifying assumptions. Details are found in Reference 3.

3.2   Re-Entry for Manned Space Capsules from Circular
       Orbit Around Earth and Lunar Return Trajectory

The configuration of the Apollo vehicle developed for lunar return is shown in Figure 2, taken from Reference 4. The capsule is still an axisymmetric blunt body, but typically it decends at some angle of attack (to a maximum of 33°) which is varied for control purposes during re-entry flight. The flow field is completely un-symmetric, thus adding a major complication to the problem. Besides the subsonic-supersonic inviscid shock layer, there is the boundary layer, and behind the body, a viscous separated region. The latter two regions interact in the viscous mixing region,

finally forming the wake which poses almost unsurmountable difficulties for a theoretical analysis. Unfortunately, because of the location of antennas, this is also an important region as far as electromagnetic wave propagation is concerned (see Section 4).

Before an analysis of the boundary layer or the wake can be made, the inviscid flow field must be known. The initial effort must, therefore, be directed toward the determination of the inviscid flow field. Since air is a rather complicated mixture of gases, especially when dissociation and ionization must be considered, a truly exact representation is not possible at the present time. In order to properly select a model, it is advantageous to consider first the conditions that are encountered along a typical re-entry trajectory in the earth's atmosphere.

In Figure 6, the cross-hatched region in the velocity-altitude diagram indicates the re-entry corridor of manned space capsules from circular orbit around Earth with about 7.9 km/sec and for lunar return with about 11.3 km/sec. Superimposed are equilibrium conditions behind a normal shock; thus the temperature, the pressure, and the density as they occur in the stagnation point region of a blunt body re-entering the earth's atmosphere can be read from the graph. Thermodynamic data for Figure 6 were taken from References 5 and 6.

It is interesting to observe that a major portion of the space vehicle trajectory is approximately parallel to a line p_s= const. The temperature lines at low velocities are practically vertical, that is, the temperature depends only on the square of the velocity. For higher velocities, the temperature depends on both velocity and altitude. The lower density of high altitudes has the effect of increasing the degree of dissociation which in turn causes a temperature decrease through the transformation of kinetic energy to energy of dissociation. Nevertheless, the stagnation temperature reaches very large values, up to $11,000^{\circ}$K in the case of lunar return.

3.3   Real Gas Effects: Molecular Vibration, Dissociation, and Ionization

During re-entry of a space vehicle through the atmosphere, extremely high velocities are encountered. For instance, at return from a lunar mission nearly parabolic velocity (11.3 km/sec), corresponding to about Mach number 35, is reached. Strong heating, starting behind the shockwave, occurs particularly in

the stagnation point region. Above Mach number 3, air no longer behaves as a perfect gas, and with increasing Mach number, molecular vibration, dissociation, and finally ionization occurs. This will change considerably the chemical composition of the air and this change will extend along the body.

A simplified presentation of the real gas effects is given in Figure 7, which illustrates various energy states of nitrogen. In addition to the well-known fact of the translational and rotational motion of the particles, we have to consider the vibrational motion of a particle for flight above Mach number 3, and initially in a limited way, the motion of the electrons within the particle. Monatomic particles have no modes of rotational or vibrational excitation. With increasing temperature the vibrations of the two atoms, within an oxygen or a nitrogen molecule, for instance, become so intense that the atoms are separated into two different particles by a collision with another body. This process is called dissociation, and it requires a considerable amount of energy, the so-called dissociation energy. For the recombination of two atoms, a triple collision is necessary, the third body carrying away the energy that the two separate atoms must release to form a stable diatomic molecule.

Ionization is the process whereby one or more electrons are removed from an atom. This process occurs when the average kinetic energy of the molecules or atoms is high enough, so that the energy transferred in a collision between two neutral atoms is sufficient to ionize one of them. The ionization (thermal) of the nitrogen atom in Figure 7 occurs only at very high temperatures. When the number of electrons in the gas, due to ionization by collision of neutral atoms, becomes appreciable, ionization by electrons may become predominant, since electrons are more efficient ionizing agents than neutral atoms. Each free moving electron that has left its shell holds an electrically negative charge. The remaining molecule is charged electrically positive in its ionized state.

3.4   Dissociation of Oxygen and Nitrogen in a Simplified Air Model

To be exact, all possible individual reactions which can occur between all components in air must be considered simultaneously. We will use the following simplified model. The model air consists of oxygen and nitrogen only. Only the dissociation of diatomic oxygen and nitrogen to monatomic oxygen and nitrogen will

be considered. Hence, reactions of oxygen with nitrogen after dissociation are neglected; in particular this means that the formation of nitric oxide, NO, is disregarded.

At a given pressure and temperature, in general only a certain fraction of the molecules are dissociated into atoms. The degree of oxygen dissociation α can be defined in various ways. We are using the following definition:

$$\alpha = \frac{m_1 (O_1)}{m_1 (O_1) + m_2 (O_2)} = \frac{\bar{n}_{O1}}{\bar{n}_{O1} + 2\bar{n}_{O2}}$$

Here α is the ratio of the mass of the atoms in the atomic state m_1 to the sum of the masses in the atomic and molecular state m_2. $\bar{n}_{O1}$ and $\bar{n}_{O2}$ are the number of particles per unit volume in the atomic or molecular state.

The degree of nitrogen dissociation is defined in the same way. Thus we obtain:

$$\beta = \frac{\bar{n}_{N1}}{\bar{n}_{N1} + 2\bar{n}_{N2}}$$

The degree of oxygen dissociation α and that of nitrogen dissociation β, as functions of temperature and pressure, are shown in Figure 8 (Ref. 3). For the calculations, thermodynamic equilibrium was assumed, and the following physical fact was considered for a further simplification. If, at a given pressure, the temperature is raised, the oxygen begins to dissociate first, and the fraction of oxygen dissociated increases with the temperature. All the while, the nitrogen practically stays in molecular form. Only after the temperature is raised to the point where the oxygen is fully (say 99%) dissociated does the dissociation of nitrogen begin. This means a separation of the two processes, which leads to two separate quadratic equations for α, the degree of oxygen dissociation, and β, the degree of nitrogen dissociation, as functions of temperature and pressure. From Figure 8, it can be seen that the dissociation for both species increases for a certain pressure with increasing temperature, and for a certain temperature with decreasing pressure.

An illustrative survey of the happenings during re-entry with respect to dissociation is given in Figure 9 (Ref. 3). The dissociation of oxygen and nitrogen at the stagnation point of a vehicle in an altitude-velocity diagram was calculated

by combination of the values given in Figure 6 and those given in Figure 8. Also included are re-entry trajectories for three ballistic vehicles from Figure 4. This diagram illustrates very well the fact that the dissociation of oxygen and nitrogen are separated from each other. There are two important restrictions in the graph. First, the dissociation values given are valid only in the stagnation point region for the respective vehicle. Second, the values are calculated for equilibrium conditions, which means assuming that the flow has sufficient time to adjust to its chemical composition due to the prevailing stagnation pressure and temperature conditions. The difference between equilibrium and non-equilibrium flow will be mentioned in Section 5. Details can be found in Reference 3.

3.5   Ionization at Re-Entry

The calculation of electromagnetic wave propagation requires the exact knowledge of the electron density in the medium. Therefore, ionization of the air must be considered as another important process during re-entry. Figure 10 (thermodynamic data from Ref. 7) shows, again for equilibrium conditions behind a normal shock, the nature of the predominant species of charged particles which must be expected in the stagnation point region of a blunt body along its re-entry trajectory. It can be seen that, almost independent of altitude, at a velocity between 5 and 7 km/sec, the only source of free electrons is the ionization of NO. Hence, all chemical reactions, which after dissociation of oxygen and nitrogen lead to the formation of nitric oxide, must be considered. In the range of velocities from 7 km/sec to 10 km/sec, atomic oxygen and nitrogen begin to ionize, and the contribution of electrons from ionization of NO declines because the fraction of NO is decreasing due to dissociation. Finally, between 10 km/sec and 12 km/sec argon begins to ionize, while atomic nitrogen and oxygen continue to become ionized.

From the discussion above, it is concluded that the following species must be considered in order to realistically approximate the electron density:

$$O_2, \; O, \; N_2, \; N, \; A, \; NO, \; NO^+, \; O^+, \; N^+, \; A^+, \; \text{and} \; e^-.$$

It can be easily seen, that the consideration of so many species means in practice a great complication of the numerical calculation. The difficulties become still larger if additional species must be considered, such as CO_2, in order to correctly

calculate the flow field when the ambient gas differs in composition from that of "Earth standard" air, as it would in other planets such as Venus and Mars.

In concluding, it must be understood that for the calculation of electron density, the simplified air model as discussed in Section 3.4 cannot be used.

4.   PLASMA EFFECTS ON COMMUNICATION AT RE-ENTRY

With re-entry from outer space into the earth's atmosphere at least technically mastered, there remains a multitude of unsolved problems, one of which is the entry-communications problem. As is well known, partial or total radio blackout is caused by the formation of a plasma sheath due to the high temperature occurring around the vehicle when entering the atmosphere. The plasma layer attenuates the transmission of electromagnetic signals from either direction.

In the most critical case, radio communication is completely blacked out. This signal blackout has already been experienced during the re-entry of the Mercury spacecraft. A much more serious condition of tracking and communication blackout is expected during the re-entry flight of the Apollo spacecraft because of the higher Apollo re-entry velocity (about 11 km/sec) in comparison to Mercury velocity (about 7 km/sec).

In order to cope with the problem, i.e., either to find some ways of propagating electromagnetic waves through the plasma or to eliminate the spurious noise, one must have not only a proper understanding of the phenomena but also a rather precise knowledge of the composition of the flow field surrounding the vehicle. The most important parameters here are the electron density, the collision frequency and the thickness of the plasma sheath in the direction of propagation.

Electron densities and collision frequencies for equilibrium conditions behind a normal shock are already available (Ref. 8) and are shown in a velocity-altitude diagram in Figure 11. The electron density is defined as the number of free electrons per unit volume. It can be observed that the electron density distribution in Figure 11 is similar to the temperature distribution in Figure 6. The given electron density distribution is valid only in the stagnation point region, because it is calculated behind a normal shock. To calculate the electron density in the antenna region is very difficult, and an accurate evaluation of the downstream

electron distribution will involve an analysis with a multitude of coupled chemical reactions.

In the range below 8 km/sec, the electron collision frequency (sec^{-1}), as shown in Figure 11, has a similar distribution to those of density and pressure (Fig. 6). In general, the average collision frequency is the average speed of the particles within a selected volume divided by the mean free path of the particles within this volume. In the data shown in Figure 11, only collisions of electrons with neutral particles or ions are considered. Electron-electron collisions are neglected.

In Figure 12, predicted blackout bounds at operational frequencies of 250 Mc, 2 kMc, and 5 kMc are presented in our well-known velocity-altitude diagram (taken from Ref. 4). Also included are three different lunar return trajectories of the Apollo vehicle and one Mercury (MA-6) trajectory for re-entry from a nearly circular orbit around the Earth. It can be seen that under the present conditions the radio communication to the earth's surface is not possible during a very important part of the re-entry. It will be particularly critical since its occurrence will coincide with the maneuver phase of the spacecraft, and it may eliminate the ground support during a vital portion of this phase or even during the entire regime of effective maneuverability depending upon the type of re-entry trajectory. More details on these problems can be found in Reference 4.

5.   HYPERSONIC FLOW OF AIR PAST BLUNT AND POINTED
       BODIES WITH NON-EQUILIBRIUM OXYGEN DISSOCIATION

5.1   Equilibrium Flow, Non-Equilibrium Flow, and Frozen Flow

Before we can discuss non-equilibrium, equilibrium, and frozen flow, we have to define thermodynamic equilibrium of a gas at rest. A gas at rest is, by definition, in thermodynamic equilibrium, if a particular volume of the gas has sufficient, or better infinite, time to bring all its internal modes of energy in equilibrium with the translational energy of the molecular motion. For our consideration those modes are molecular vibration, dissociation, electronic excitation, and ionization.

Now considering flow processes of a gas, it is obvious that equilibrium flow is only one limiting case, namely when the changes of the state of the gas flowing

along a streamline are so slow that at any point equilibrium is obtained, or stated more exactly, equilibrium is very closely approached. At hypersonic velocities, the time available is, in general, too short for the gas particles which are undergoing rapid density, temperature, and composition changes to reach thermodynamic equilibrium. Hence, in general, we have non-equilibrium flow. The degree of molecular vibration, the degree of dissociation (chemical composition), and the degree of ionization will still change from point to point along the streamline but will not reach thermodynamic equilibrium at any point.

Another limiting case occurs when the gas moves so fast that the internal energy modes have no time to follow the changing density and temperature with the result that the vibrational energy, the energy in dissociation, and the energy in ionization stay very nearly constant. We call this flow frozen; the gas might be vibrationally frozen, and/or chemically frozen (frozen dissociation or no change in degree of dissociation), and/or the gas has frozen ionization.

This qualitative discussion demonstrates that calculation of hypersonic flow obviously requires very complex thermodynamic relations which include the above mentioned real gas effects and the intermediate reactions and products. Finally , without interpretation at this place, the important fact should be noted that non-equilibrium flow fields are dependent on the absolute size of the body and therefore they are generally not similar for geometrically similar bodies even at completely equal free stream conditions.

5.2 Some Results of Hypersonic Flow Past a Circular Cylinder, a Sphere, and a Circular Cone

For non-equilibrium flow field calculations, the properties behind the shock are mostly calculated on the basis of frozen composition (at the free stream value) across the shock, but with molecular vibrations and rotations in equilibrium with the translational temperature. The conditions behind the shock, serving as boundary and initial values for the flow field calculations, are calculated on the basis of conservation of mass, momentum and energy across the shock.

Some results of our investigations at the University of Alabama Research Institute are shown starting with Figure 13. Using Dorodnitsyn's method of integral relations, hypersonic chemically relaxing inviscid flow of air past a circular cylinder

has been calculated. The effects of non-equilibrium oxygen dissociation on the distribution of the flow variables in the subsonic and supersonic region of the shock layer were considered. The influence of oxygen dissociation in the free stream on the shock detachment distance and the flow field in general was also investigated.

Shock waves in front of a cylinder with the body radius 0.1 m at four different Mach numbers from 3.0 to 14.2 are shown in Figure 13. The shock detachment distance decreases from approximately 0.7 to 0.2 of the body radius with increasing Mach number. Included are the sonic points on the body surface which move toward the stagnation point with increasing Mach number. Figure 13 also shows that the shock shape deviates considerably from a concentric circle, even where the velocity in the shock layer is still subsonic.

The shock detachment distance and the sonic point location as functions of the free stream Mach number are presented in Figure 14. Non-equilibrium flow results from Reference 9 with and without free stream dissociation ($\alpha_1 = 0.5$; $\alpha_1 = 0$) are compared with perfect gas results ($\gamma = 1.4$) from References 10 and 11.

It is already well known from perfect gas calculations that with increasing free stream Mach numbers the bow shock moves closer to the body. It is seen from Figure 14 that in chemical non-equilibrium flow this trend is retained. Figure 14 also indicates clearly that dissociation of the free stream, keeping all other free stream parameters unchanged, causes the bow shock to move away from the body. One reason for this effect is that, for a dissociated free stream, the density behind the shock is lower than for corresponding conditions without free stream dissociation. The effect is seen to increase with decreasing free stream Mach number.

Also from Figure 14 it is observed that the calculations from Reference 9 yield a stagnation shock detachment distance which is much smaller, even for an undissociated free stream, than the values obtained from perfect gas calculations. Responsible for this effect is the inclusion of vibrational excitation into our calculation throughout the flow field. The molecular vibration is assumed to be in equilibrium. It is shown that, for a free stream Mach number of $M_1 = 3$, where the bow shock does not yet cause appreciable molecular vibration in the shock layer, the non-equilibrium flow calculation predicts a value which is very close to the known perfect gas result.

A comparison of the shock stand-off-distance between cylinder and sphere is presented in Figure 15. The result for the cylinder is taken from Reference 9, that for the sphere from Reference 12. The free stream conditions in both cases are not the same, and other results are not available at the present time. The fact, that in case of the sphere the shock moves closer to the body, will be true also for identical free stream conditions. However, the location of the sonic point is very sensitive, thus one cannot compare the two bodies at different free stream conditions with respect to the sonic point location .

Finally, Figure 16 shows the shock layer thickness for chemically and vibrationally frozen flow past a circular cone (Ref. 13). Included is the effect of free stream oxygen dissociation at three Mach numbers. It can be seen that also in case of the cone as with the cylinder, the shock layer thickness decreases with increasing Mach number, and increases with increasing free stream dissociation. The behavior of the shock layer thickness with regard to the cone angle shows a pronounced minimum which, with increasing Mach number, moves to smaller cone angle; obviously the minimum for Mach number 20 lies left of the region covered by our calculation.

All the results in Figure 16 for chemically and vibrationally frozen flow around a circular cone are independent of the free stream density and body size (cone length), and the shock shape represents again an axisymmetric cone. The results for non-equilibrium flow are more complicated and are discussed in detail in References 13 and 14. In this case, for instance, the free stream density and the cone length have influence on the flow field, and the shock no longer has a conical shape.

6.   SUMMARY

One of the most important problems in astronautics today is to return manned and unmanned satellites and space vehicles structurally intact. During re-entry of such vehicles into the atmosphere, extremely high velocities are encountered. At return from a lunar mission, for instance, nearly parabolic velocity of 11.3 km/sec is reached, which corresponds to about Mach number 35, causing high stagnation temperatures with a maximum of 11,000°K at 60 km altitude. Already at much smaller velocities, namely for flight above Mach number 3, air no longer behaves as a perfect gas; and molecular vibration, dissociation, and ionization occur, absorbing large amounts of energy.

The presentation of the re-entry trajectories in a velocity-altitude diagram is of great importance, in order to determine free stream conditions as well as the conditions in the stagnation point region of the re-entering vehicle. Also, the degree of dissociation and some characteristics of ionization are usefully shown as parameters in velocity-altitude diagrams.

Radio communication blackout during an important portion at re-entry is caused due to difficulties encountered with the propagation of electromagnetic waves. These problems are associated with the electron density and collision frequency of the free electrons in the plasma sheath. They are significant at high enthalpy flow which is dissociated and ionized and generally in non-equilibrium both in the shock layer and in the wake.

Results of calculations using the Integral Method for hypersonic flow of air with non-equilibrium oxygen dissociation are presented. A circular cylinder and a sphere were investigated up to Mach number 14, and a circular cone up to Mach number 20. In case of the cylinder and the cone, calculations assuming dissociation of the free stream were included. It was found that the shock wave moves closer to those bodies with increasing Mach number, but with rising free stream dissociation at otherwise fixed conditions, the shock wave moves away from the body.

7. REFERENCES

1. U.S. Standard Atmosphere, 1962. U.S. Government Printing Office, Washington 25, D.C.

2. USAF Cambridge Research Center: Atmospheric models. Document #56 SD 233, reproduced by General Electric, Missile and Ordnance System Dept., 1956.

3. Hermann, R., "Hypersonic Flow Problems During Re-Entry Into the Atmosphere," Yearbook 1961, Wissenschaftliche Gesellschaft fuer Luftfahrt, Friedr. Vieweg & Sohn, Braunschweig, Germany, 1961.

4. Lehnert, R., Rosenbaum, B., "Plasma Effects on Appollo Re-Entry Communications," Report X-515-64-8, Goddard Space Flight Center, Greenbelt, Md., Jan. 1964.

5. Wittliff, C.E., Curtis, J.T., "Normal Shock Wave Parameters in Equilibrium Air," Cornell Aero. Lab., CAL Report No. CAL-111, Nov. 1961.

6. Marrone, P.V., "Normal Shock Waves in Air: Equilibrium Composition and Flow Parameters for Velocities from 26,000 to 50,000 ft/sec," Cornell Aero. Lab., CAL Report No. AG-1729-A-2, August 1962.

7. "The Thermodynamic Properties of High Temperature Air," Chance Vought Research Center, Report No. RE-1R-14, June 1961.

8. Huber, P.W., "Hypersonic Shock-Heated Flow Parameters for Velocities to 46,000 ft/sec and Altitudes to 323,000 ft," NASA TR R-163, December 1963.

9. Hermann, R., Thoenes, J., "Hypersonic Flow of Air Past a Circular Cylinder With Non-Equilibrium Oxygen Dissociation Including Dissociation of the Free Stream." Paper presented at the VI. European Aeronautical Congress at Munich, Germany, Sept. 1965. To be published in the Yearbook 1965, Wissenschaftliche Gesellschaft fuer Luft-und Raumfahrt, Friedr. Vieweg & Sohn, Braunschweig, Germany, 1965. Also University of Alabama Research Institute, Huntsville, UARI Research Report No. 28, September 1965.

10. Belotserkovskii, O.M., "Flow Past a Circular Cylinder With a Detached Shock Wave," Doklady Akad. Nauk SSSR 113, No. 3, 1957.

11. Archer, R.D., "Inviscid Supersonic Flow Around an Elliptic Nose," Ph.D. Thesis, University of Minnesota, November 1963 (Adviser: R. Hermann).

12. Shih, W.C.L., Baron, J.R., Krupp, R.S., and Towle, W.J., "Nonequilibrium Blunt Body Flow Using the Method of Integral Relations," Mass. Institute of Technology, DDC ADNJ 415934, May 1963.

13. Thoenes, J., "Inviscid High Temperature Hypersonic Flow of Air Past Pointed Bodies of Revolution," University of Alabama Research Institute, Huntsville, UARI Research Report No. 25, May 1965, supported by the U. S. Army Missile Command under Contract No. DA-01-009-AMC-166 (Z).

14. Herman, R., "Hypersonic Non-Equilibrium Flow and its Thermodynamic Relations," Invited lecture presented at the 4. Space Symposium at the University of Goettingen, Germany, Oct. 18-22, 1965. Also University of Alabama Research Institute, Huntsville, UARI Research Report No. 30, November, 1965.
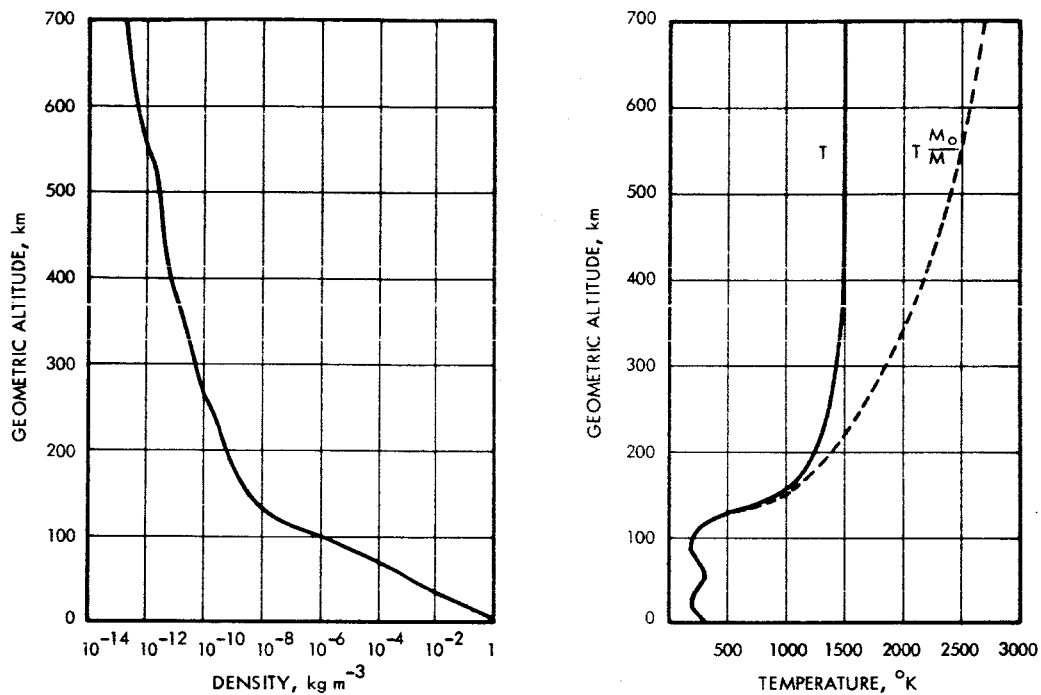
FIG. 1. DENSITY ρ AND TEMPERATURE T AS FUNCTIONS OF GEOMETRIC ALTITUDE Z.
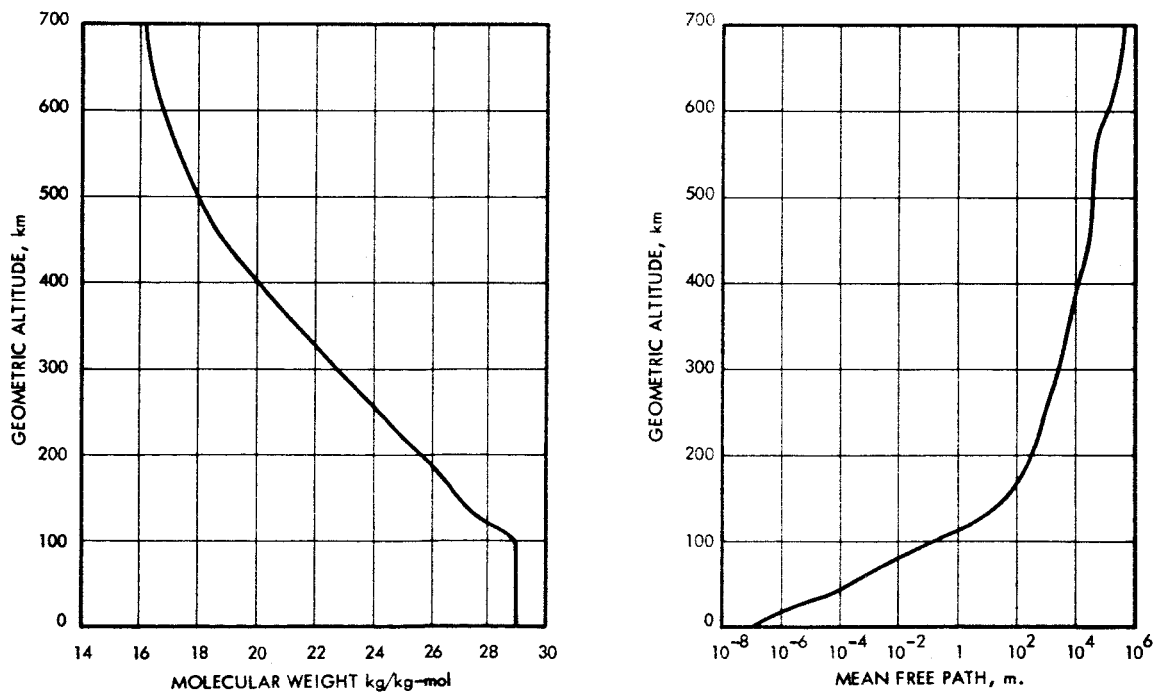U. S. STANDARD ATMOSPHERE, 1962, REF. 1.

FIG. 2. MOLECULAR WEIGHT M AND MEAN FREE PATH L AS FUNCTIONS OF GEOMETRIC ALTITUDE Z.
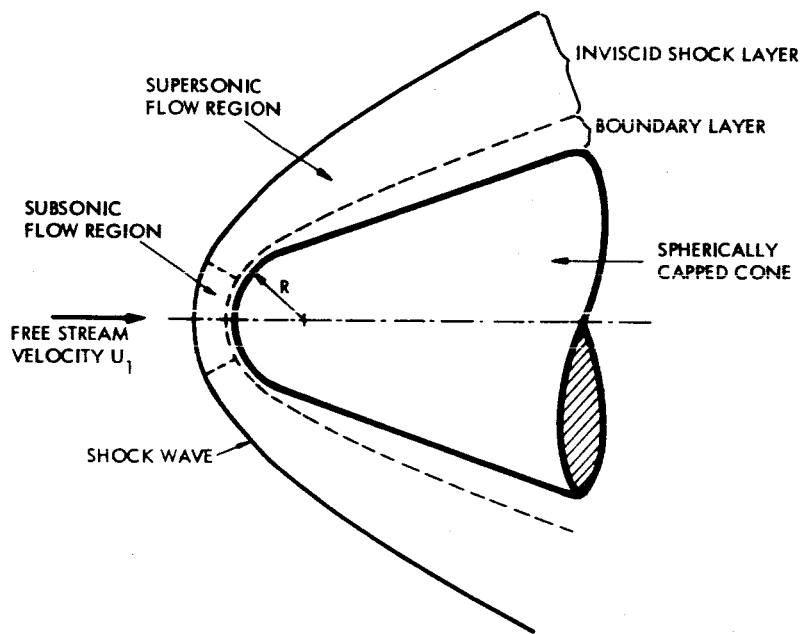U. S. STANDARD ATMOSPHERE, 1962, REF. 1.

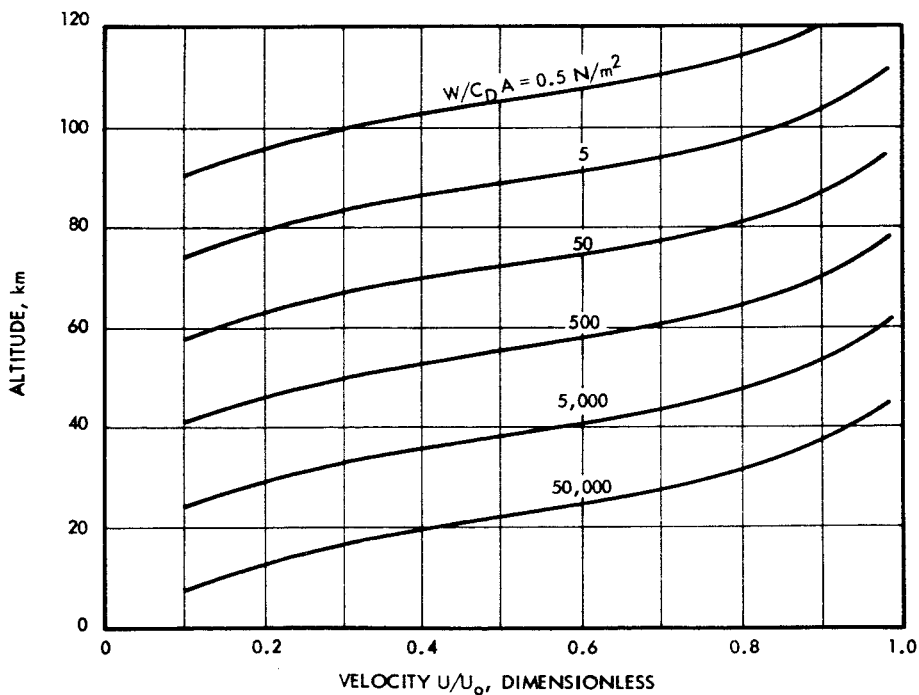FIG. 3. BLUNT BODY CONFIGURATION AND FLOW FIELD (SCHEMATIC).

FIG. 4. RE-ENTRY TRAJECTORIES FOR BALLISTIC VEHICLES
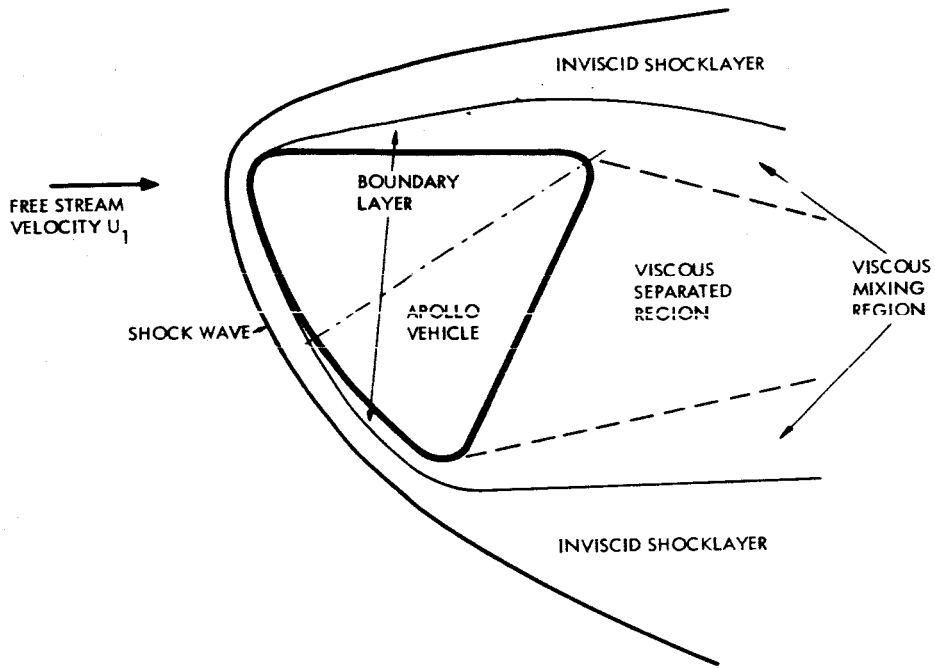IN EARTH ATMOSPHERE FROM CIRCULAR ORBIT ($U_o = 7,910$ m/s).
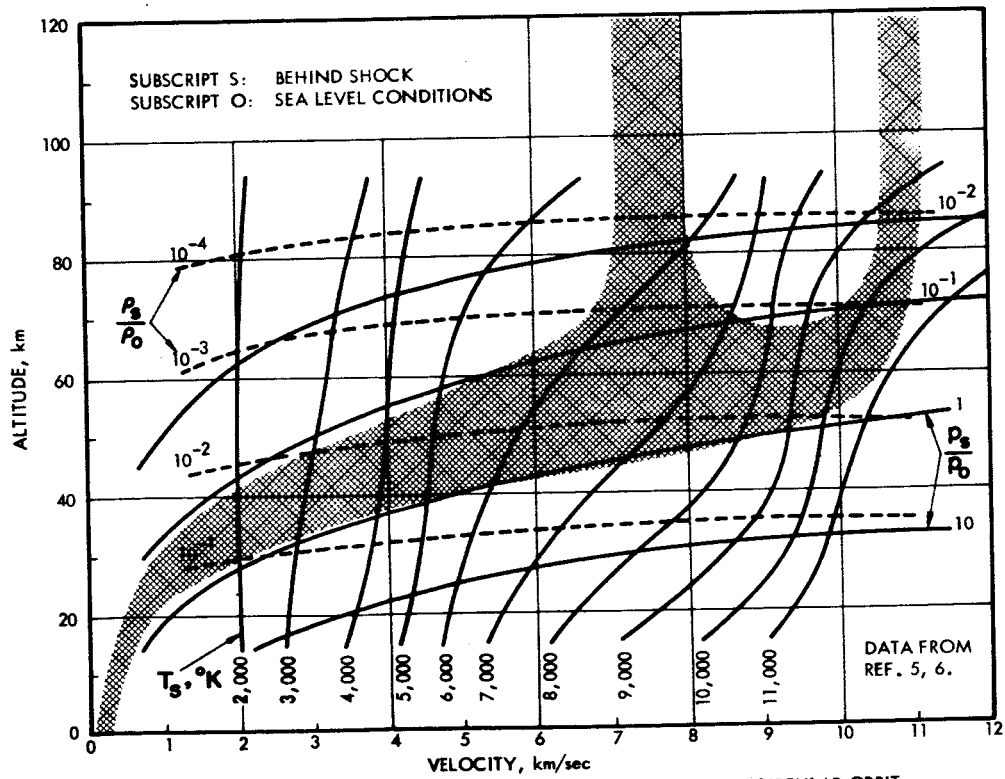
FIG. 5. HYPERSONIC FLOW REGIONS (SCHEMATIC) FOR APOLLO VEHICLE, REF.4.

FIG. 6. FLIGHT REGION OF MANNED RE-ENTRY VEHICLES FROM CIRCULAR ORBIT AND LUNAR RETURN. ALSO EQUILIBRIUM CONDITIONS BEHIND A NORMAL SHOCK.
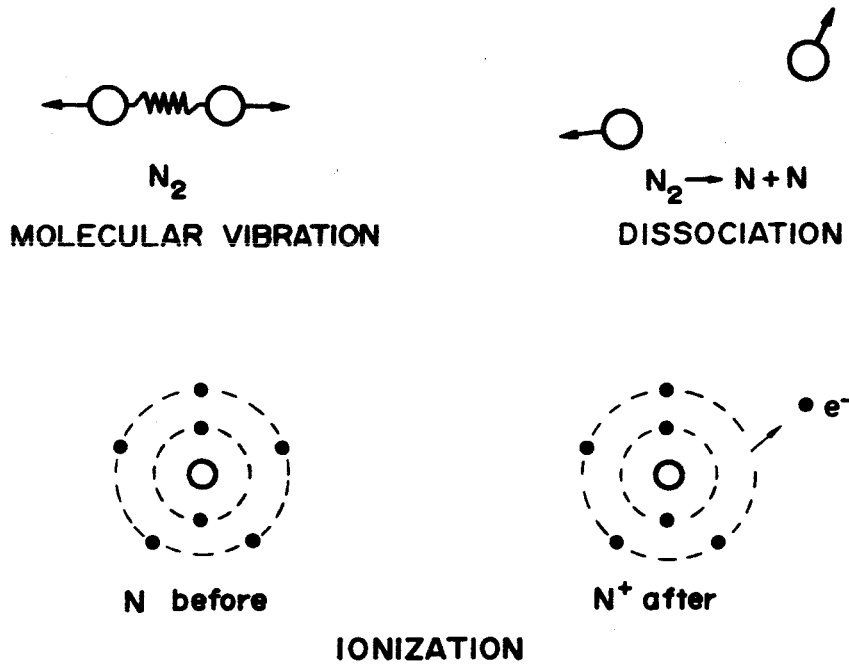
FIG. 7. ENERGY STATES OF NITROGEN.
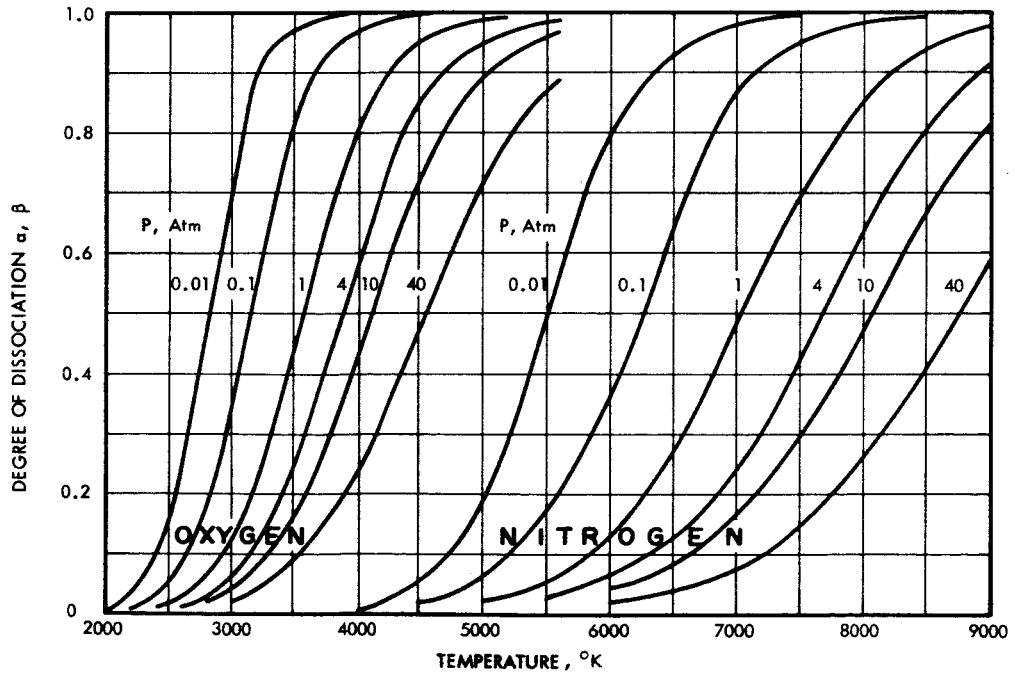
FIG. 8. DEGREE OF OXYGEN DISSOCIATION α AND NITROGEN DISSOCIATION β AS FUNCTION OF
TEMPERATURE AND PRESSURE, CALCULATED FOR SIMPLIFIED AIR–MODEL IN EQUILIBRIUM.
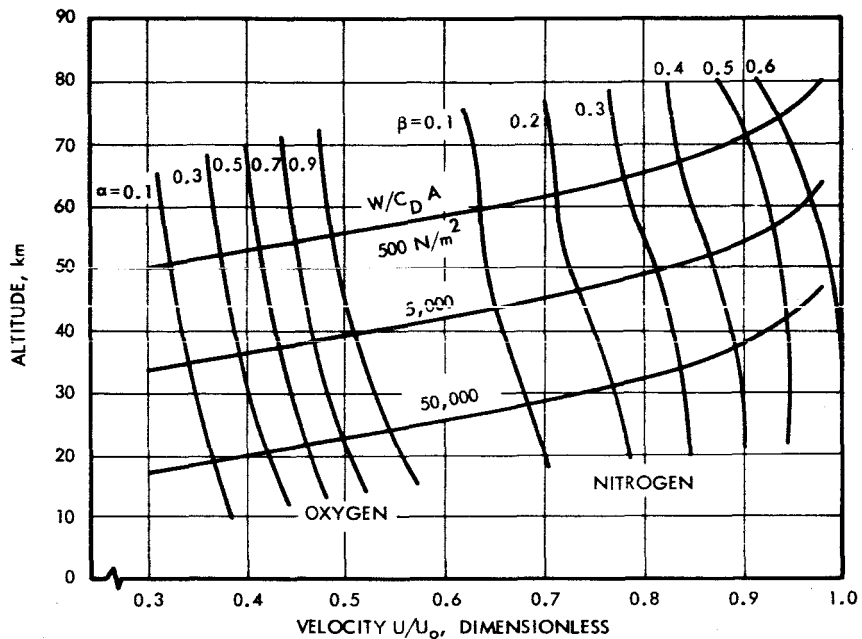
FIG. 9. DEGREE OF OXYGEN AND NITROGEN DISSOCIATION FOR SIMPLIFIED AIR-MODEL AT
STAGNATION POINT. ALSO RE-ENTRY TRAJECTORIES FOR VARIOUS BALLISTIC VEHICLES.
CIRCULAR VELOCITY U_o = 7,910 m/s.
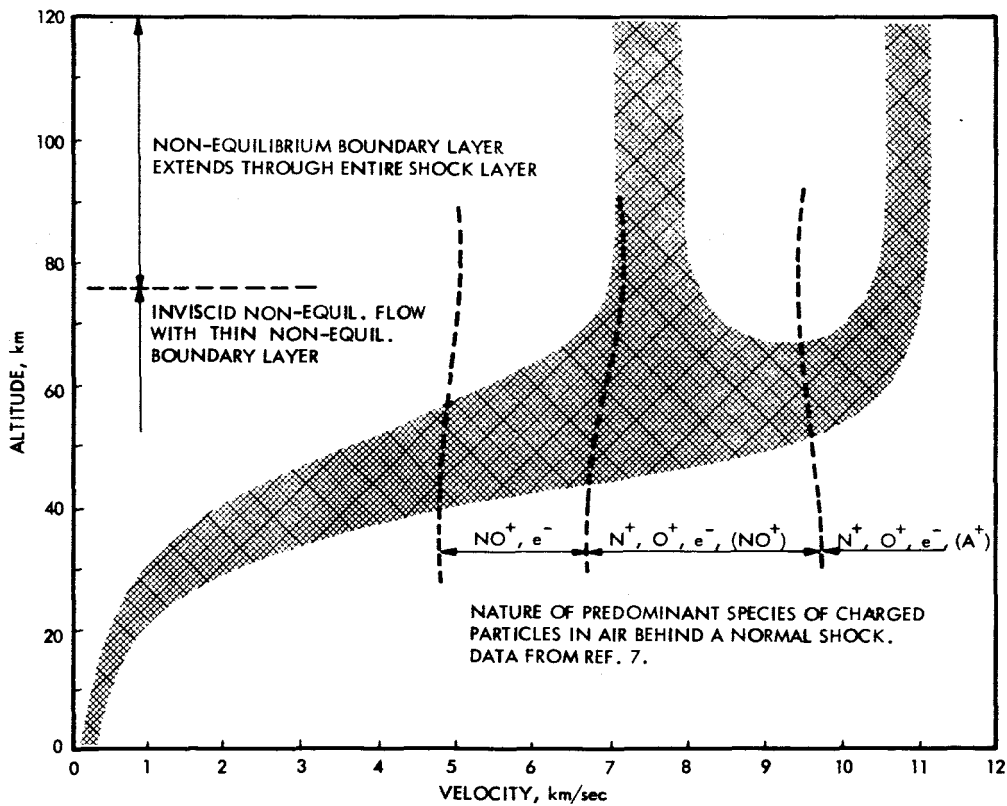
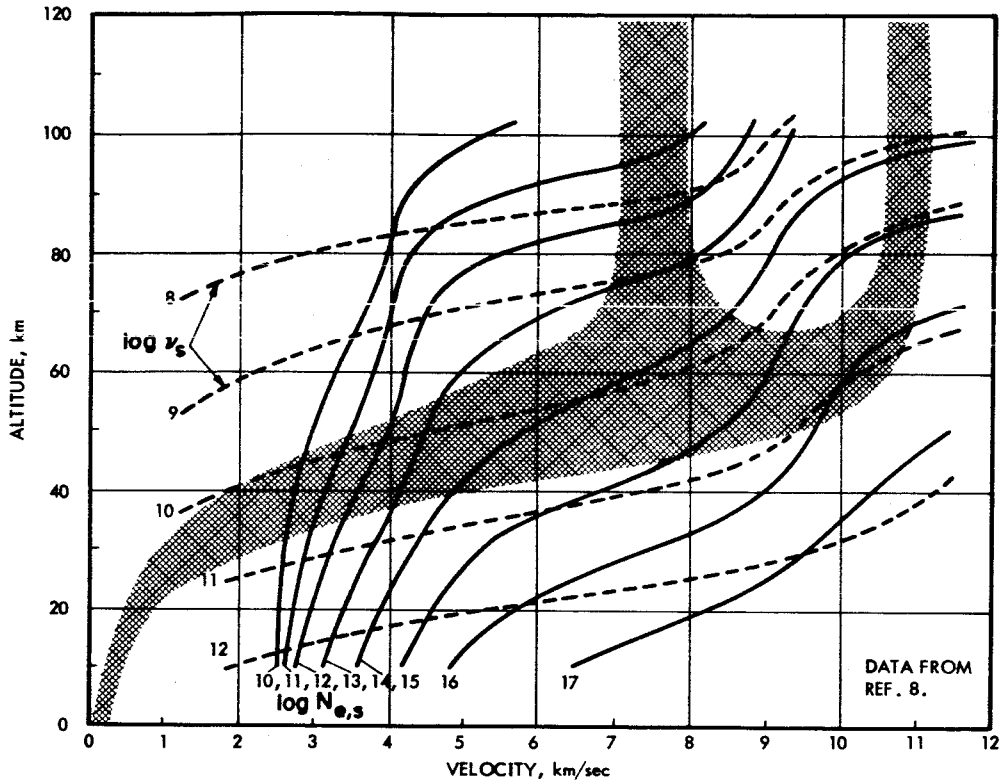FIG. 10. NATURE OF CHARGED PARTICLES FOR EQUILIBRIUM CONDITIONS BEHIND A NORMAL SHOCK.

FIG. 11. ELECTRON DENSITY N_e, cm^{-3}, AND COLLISION FREQUENCY ν, sec^{-1}, FOR EQUILIBRIUM CONDITIONS BEHIND A NORMAL SHOCK DURING RE-ENTRY IN EARTH ATMOSPHERE.
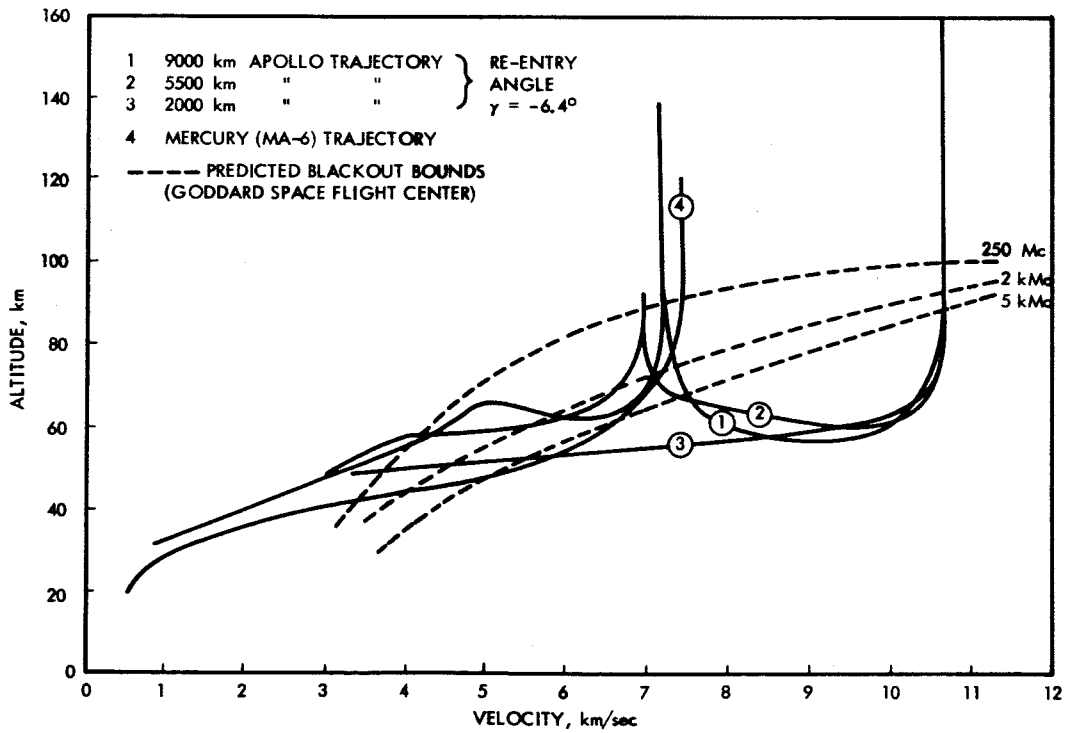

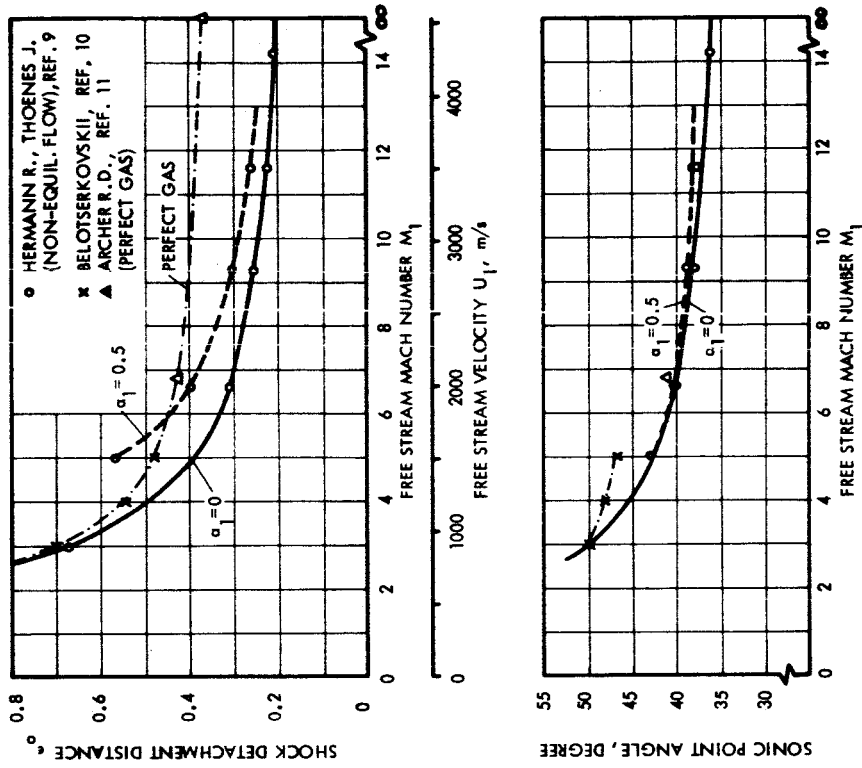FIG. 12. BLACKOUT BOUNDS OF TYPICAL MERCURY AND APOLLO RE-ENTRY TRAJECTORIES (REF. 4).

22

FIG. 14. SHOCK DETACHMENT DISTANCE AND SONIC POINT ANGLE AT VARIOUS MACH NUMBERS FOR A CIRCULAR CYLINDER. BODY RADIUS 0.1 m; CONDITIONS IN 30 km ALTITUDE.
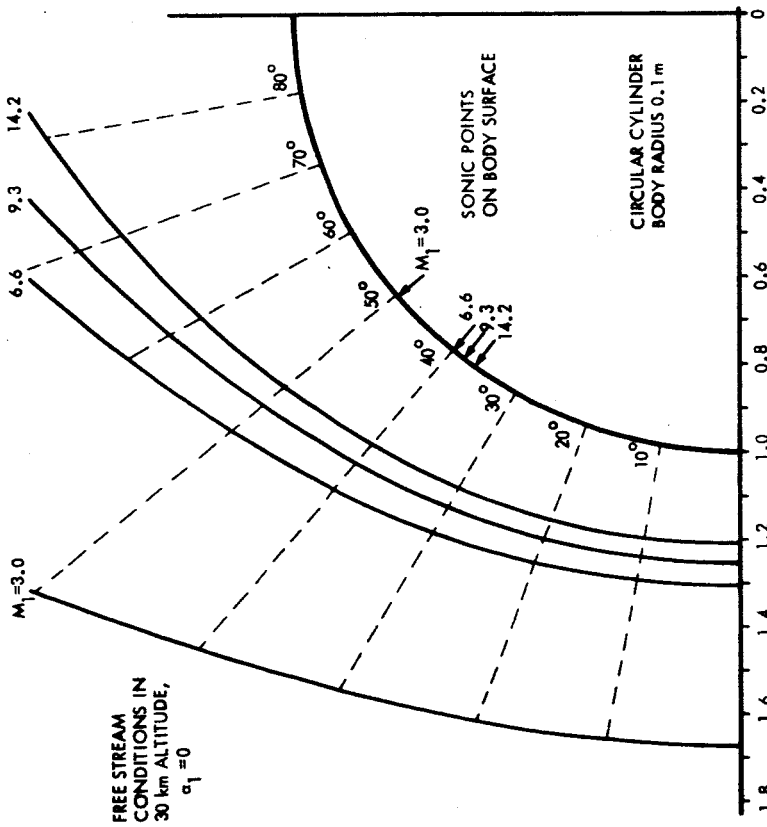
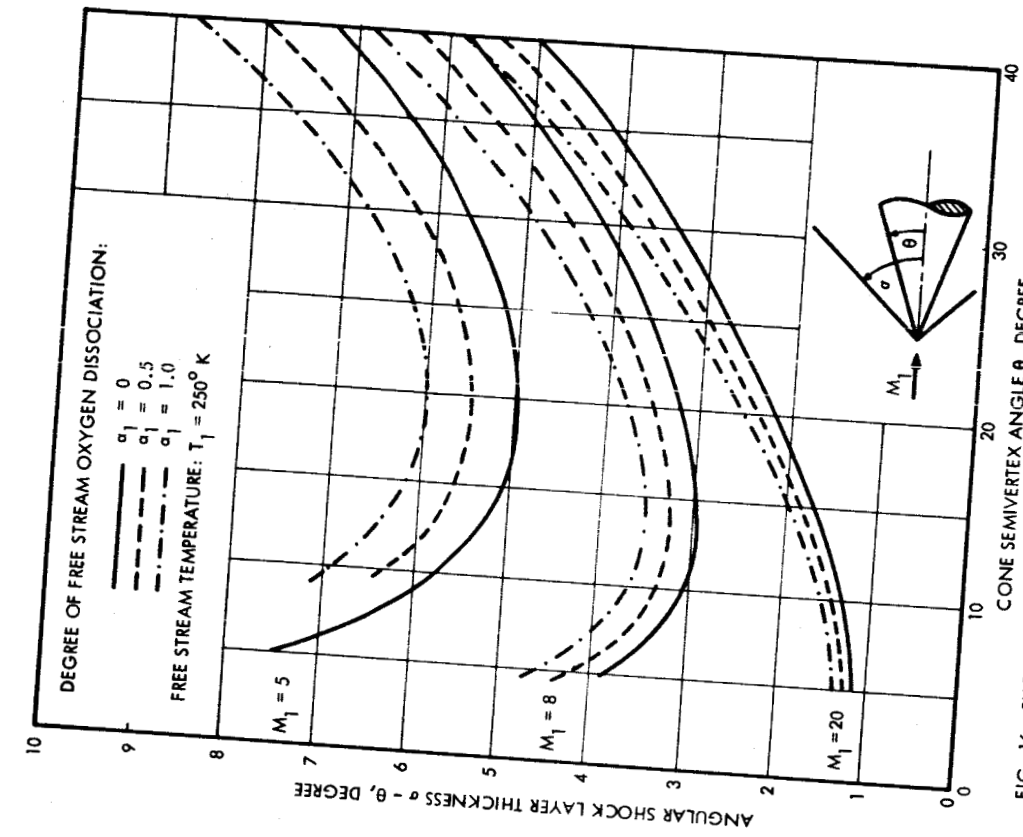FIG. 13. SHOCK WAVES IN FRONT OF A CYLINDER FOR 4 MACH NUMBERS (NON-EQUILIBRIUM FLOW).

FIG. 16. SHOCK LAYER THICKNESS AS FUNCTION OF CONE SEMIVERTEX ANGLE FOR CHEMICALLY AND VIBRATIONALLY FROZEN FLOW AROUND A CIRCULAR CONE. INCLUDED IS FREE STREAM OXYGEN DISSOCIATION AT 3 MACH NUMBERS.

CIRCULAR CYLINDER
BODY RADIUS 0.1 m
$M_1 = 14.2$; $a_1 = 0$
ALTITUDE 30 km

REFERENCE 9

SPHERE
BODY RADIUS 0.3 m
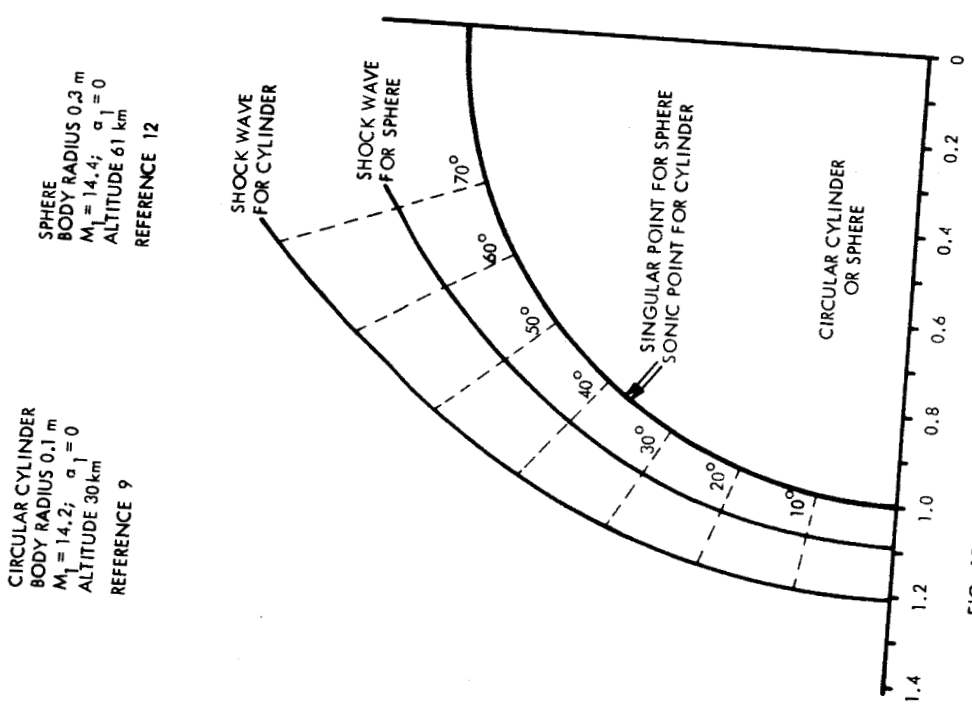$M_1 = 14.4$; $a_1 = 0$
ALTITUDE 61 km

REFERENCE 12

FIG. 15. SHOCK WAVES IN FRONT OF A CYLINDER AND A SPHERE FOR NON-EQUILIBRIUM FLOW.